RA'EGA
O ESPAÇO GEOGRÁFICO EM ANÁLISE
https://revistas.ufpr.br/raega

ISSN eletrônico 2177-2738
RA'EGA, Curitiba, PR, V.65, n.1, p. 137–156, 4/2026
http://dx.doi.org/10.5380/raega.v65i1.103485

Land Surface Temperature in Itapetininga, São Paulo State, Brazil: Seasonal and Inter-annual Variability under Land Use and Land Cover Changes (2003–2023)

Temperatura de Superfície Terrestre em Itapetininga – SP: variabilidade sazonal e interanual sob mudanças no uso e cobertura da terra (2003–2023)

Camila Reigota [*], Rafael Zini Ouriques [*], Greisi Aline de Azeredo [*], Waterloo Pereira Filho [*]

[*]Department of Geosciences, Federal University of Santa Maria – Main Campus, reigotacamila794@gmail.com; rafaziniouriques@gmail.com; azeredo.gre@gmail.com; waterloopf@gmail.com

http://dx.doi.org/10.5380/raega.v65i1.103485

Abstract

Land use and land cover (LULC) transformations, due to urban growth and agro-forestry-pastoral activities, have caused changes in the surface energy balance. In this context, the variation of Land Surface Temperature (LST) in the Itapetininga municipality Itapetininga, São Paulo State, from 2003 to 2023, was analyzed in relation to the Normalized Difference Vegetation Index (NDVI) and Land Use/Land Cover, Data from the Moderate Resolution Imaging Spectroradiometer (MODIS) and the MapBiomas Project were used. An increase of NDVI and a decline of LST were observed over the 21-year period analyzed. The regulatory effect of vegetation on LST was confirmed by the Mann–Kendall and Sen's Slope trend tests, as well as by the Spearman and Mann–Kendall correlation analysis. A statistically significant trend was observed only for NDVI ($\tau = 0.1359$; $p < 0.001$). The relationship between the variables showed a negative and significant correlation ($\rho = –0.50$; $\tau = –0.36$). The Shapiro–Wilk normality test indicated that the data distribution does not meet parametric assumptions, justifying the use of nonparametric statistical methods. Furthermore, LULC changes between 2003 and 2023 revealed the expansion of agriculture (8.86%), reforestation (6%), and forest (0.69%), contributed, in part, to the decline in LST. Reforestation stood out as an important thermal mitigator, although its isolated influence still depends on specific analysis. It is concluded that the local thermal dynamics results from the interaction between climatic indicators and anthropogenic changes, reinforcing the importance of integrated monitoring using orbital and ground-based data to support territorial planning and climate adaptation strategies.

Keywords:
Remote Sensing, Normalized Difference Vegetation Index, Extreme thermal events.

ISSN eletrônico 2177-2738
RA'EGA, Curitiba, PR, V.65, n.1, p. 137–156, 4/2026
http://dx.doi.org/10.5380/raega.v65i1.103485

Resumo

As transformações no uso e cobertura da terra (*Land Use and Land Cover* – LULC), impulsionadas pela expansão urbana e atividades agrossilvipastoris, têm provocado alterações no balanço de energia à superfície. Neste sentido foi analisada a variação da Temperatura da Superfície Terrestre (TST) no município de Itapetininga – SP no período de 2003 a 2023, associada ao *Normalized Difference Vegetation Index* (NDVI) e LULC. Utilizou-se dados do *Moderate Resolution Imaging Spectroradiometer* (MODIS) e do projeto MapBiomas. Verificou-se o aumento do NDVI e o declínio da TST ao longo destes 21 anos. O efeito regulador da vegetação na TST foi confirmado pelos testes de tendência de Mann-Kendall e Sen's Slope e pelas análises de correlação de Spearman e Mann-Kendall. Observou-se tendência estatisticamente significativa apenas para o NDVI ($\tau = 0{,}1359$; $p < 0{,}001$). A relação das variáveis apresentou correlação negativa e significativa ($\rho = -0{,}50$; $\tau = -0{,}36$). O teste de normalidade de Shapiro-Wilk indicou que a distribuição dos dados não atende aos pressupostos paramétricos, ao justificar o uso de métodos estatísticos não paramétricos. Ainda, as mudanças no LULC (2003 e 2023) mostraram a expansão da agricultura (8,86%), silvicultura (6%) e floresta (0,69%), contribuindo, em parte, para o declínio da TST. A silvicultura destacou-se como mitigadora térmica, embora sua influência isolada ainda dependa de análises específicas. Conclui-se que a dinâmica térmica local resulta da interação de indicadores climáticos e mudanças antrópicas, o que reforça a importância do monitoramento integrado de dados orbitais e terrestres, para auxiliar estratégias de ordenamento territorial e adaptação climática.

Palavras-chave:
Sensoriamento Remoto, *Normalized Difference Vegetation Index,* Eventos térmicos extremos.

I. INTRODUCTION

There is a strong increase on the use of geo-technologies to obtain information about the terrestrial environment, through the use of urban climate indicators and Land Use and Land Cover (LULC) indicators, such as Land Surface Temperature (LST) and the Normalized Difference Vegetation Index (NDVI) (Norton et al., 2015; Hendges; Follador; Andres, 2020; Kara; Yavuz, 2025). These indicators can be determined with remote sensing data, obtained by sensors on board satellites that operate in different regions of the electromagnetic spectrum, such as thermal infrared, which is widely used for urban climate studies (Coelho; Corrêa, 2013; Oke et al., 2017; Porangaba; Amorim, 2019; Romero et al., 2020).

The urbanization process is one of the main factors impacting the local climate, as it is related to changes in the LULC (Oke et al., 2017). The use of highly reflective structures and building materials (e.g. concrete, asphalt, roof tiles) alters the propagation of incident solar radiation in urban areas, resulting in diverse microclimates, potentially forming urban heat islands. (Mashiki; Campos, 2013). Most of these structures in

ISSN eletrônico 2177-2738
RA'EGA, Curitiba, PR, V.65, n.1, p. 137–156, 4/2026
http://dx.doi.org/10.5380/raega.v65i1.103485

cities have dark tones, so they reflect less and absorb more radiation compared to materials found in natural environments (Hung et al., 2006; Oke et al., 2017).

Urban elements, along with the emission of heat, humidity, and pollutants, alter the exchange of energy and moisture between the surface and the atmosphere (Hung et al., 2006; Sousa; Ferreira, 2012). Thus, in built environments, indicators related to urban climate, such as surface temperature and air temperature (Tar), are higher near the surface compared to the temperatures of neighboring natural areas (Flores; Pereira Filho; Karam, 2016). Urban growth is one of the main factors in the suppression of forest areas in several regions of the country (Amorim et al., 2017). In addition to the increase of urban centers, agricultural activities result in alterations to natural vegetation and, consequently, an increase in LST (Amorim et al., 2017; Xiong et al., 2012; Gavsker, 2023). Thus, the influence of LULC type on LST variation is consistently reported in studies conducted in different locations (Romero et al., 2020; Flores; Pereira Filho; Karam, 2016; Kara; Yavuz, 2025).

Furthermore, the risk due to high temperatures in urban environments is closely linked to vulnerability trends and exposure levels of the population (IPCC, 2023). The temperature of urban centers is generally higher than the temperature of rural environments, with the predominance of asphalt pavement, vertical buildings, and lack of vegetation cover (Santos; Teixeira; Almeida, 2019). Those most vulnerable to these negative effects are the elderly, children, people with chronic diseases, low-income populations, and those who work outdoors (Norton et al., 2015). In addition, extreme weather events correspond to conditions in which meteorological variables (rainfall – PP and air temperature – Tar) show deviations from the expected climatological pattern for a given region, in intensity and duration. These events include droughts, floods, and heat waves, frequently linked to large-scale atmospheric circulation patterns, such as El Niño and La Niña (Dias, 2014).

Rao (1972) was the first to demonstrate that urban areas could be identified through analysis of thermal infrared data acquired by a satellite. Similarly, Lombardo (1985) was a pioneer in Brazil to use NOAA/AVHRR satellite images for the identification of the surface temperature in downtown São Paulo city. This author found peaks of 25 °C in contrast to the densely vegetated adjacent areas. Recently, Kara and Yavuz (2025) observed trends in surface temperature variation in São Paulo, with differences between the urban center and neighboring regions, especially in the North of the State. These results highlight the influence of changes in the LULC (Low Limit Temperature), associated with agricultural expansion and reduced vegetation cover.

Although several studies investigated the relationship between surface temperature (ST) and changes in the local land use (LULC) in São Paulo city and adjacent regions (Amorim, 2017; Porangaba; Amorim, 2019; Romero et al., 2020; Milantoni; Toledo, 2022; Kara; Yavuz, 2025), there is a scarcity of works specifically focused

ISSN eletrônico 2177-2738
RA'EGA, Curitiba, PR, V.65, n.1, p. 137–156, 4/2026
http://dx.doi.org/10.5380/raega.v65i1.103485

on the Itapetininga municipality. In this context, a gap persists to understand how anthropogenic transformations that have occurred over two decades, especially those linked to urban expansion, agricultural activities, and forestry, have influenced the intensification or attenuation of local thermal dynamics. Therefore, the challenge is to assess to what extent these spatial-temporal changes in the LULC were determinants for the variation in LST in the study area. Thus, the objective of this article is to analyze the variation in LST and its relationship with NDVI and LULC in the municipality of Itapetininga, São Paulo State, from 2003 to 2023.

II. Materials and Methods

Study Area

The study area is the Itapetininga municipality, in SW São Paulo State (Geographical coordinates 23°35'08.0"S; 48°02'51.0"W), with a territorial area of 1,792,08 km², of which 81.72 km² correspond to urban area and 1,710,36 km² to the rural area. Itapetininga is localized in the transition zone between the interior of São Paulo and the influence of the Serra do Mar/Paraná mountain range (Figure 1).

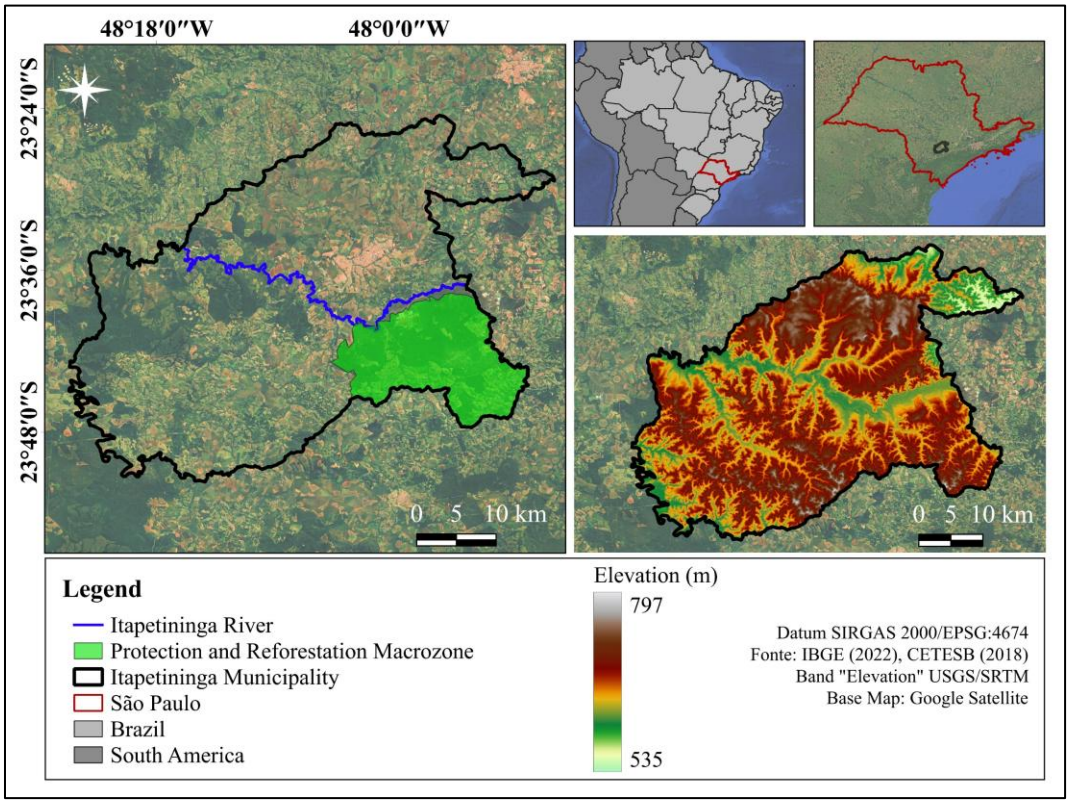

Figure 1 – Localization of study area – Itapetininga / São Paulo State.

The municipality is located within the Upper Paranapanema Hydrographic Basin, at the Itapetininga River. It borders the municipalities of Guareí and Tatuí to the North, Capão Bonito, São Miguel Arcanjo, and Pilar

ISSN eletrônico 2177-2738
RA'EGA, Curitiba, PR, V.65, n.1, p. 137–156, 4/2026
http://dx.doi.org/10.5380/raega.v65i1.103485

do Sul to the South, Alambari, Capela do Alto, and Sarapuí to the East, and Campina do Monte Alegre, Angatuba, and Buri to the West (PMMAeC, 2023). Its estimated population is 164,256 inhabitants in 2025 (IBGE, 2025). Itapetininga is the third largest municipality in the São Paulo State regarding territorial extension. According to the Köppen classification, the climate is humid subtropical (Cfa), with an average annual rainfall of 1,240 mm, concentrated from October to March (spring-summer), and a drier period from April to September (autumn-winter). Similarly, the average monthly temperature also shows a pattern throughout the year, with minimum temperatures close to 15 °C in the months of April to September, and maximum values around 26 °C in the months of October to March (PMDRS, 2025).

The municipality's elevation varies from 535 m to 797 m, with an average altitude of 670 m. The terrain is characterized by hillocks, mountains, and floodplains, with straight, concave, or gently convex slopes, frequently associated with headwater amphitheaters (CPRM, 2015). In this sense, among the municipalities of São Paulo State, it ranks 1st in arable land, highlighting its great potential for growth in this sector (PMDRS, 2025). Agroforestry production is favored by crops such as eucalyptus, oranges, broiler chickens, potatoes, sugarcane, corn, and cattle. Furthermore, the region has the Itapetininga Experimental Station, located in the eastern part of the municipality, within the Protection and Reforestation Macrozone (PRM), which houses experimental and commercial plantations of *Pinus elliottii*, with a total area of 6,706 ha, of which 3,026 ha correspond to areas with native vegetation and 3.680 ha comprise areas of exotic *Pinus elliottii* trees (SEMIL, 2025).

Data and Methods

The study was divided in two stages: 1st. Construction of a Database and Data Processing; and 2nd. Statistics and Spatial-temporal Analysis, as shown in Figure 2. The first stage corresponds to obtain the data and the products used for each variable, while the second one addresses the methods and statistics used to achieve the result.

ISSN eletrônico 2177-2738
RA'EGA, Curitiba, PR, V.65, n.1, p. 137–156, 4/2026
http://dx.doi.org/10.5380/raega.v65i1.103485

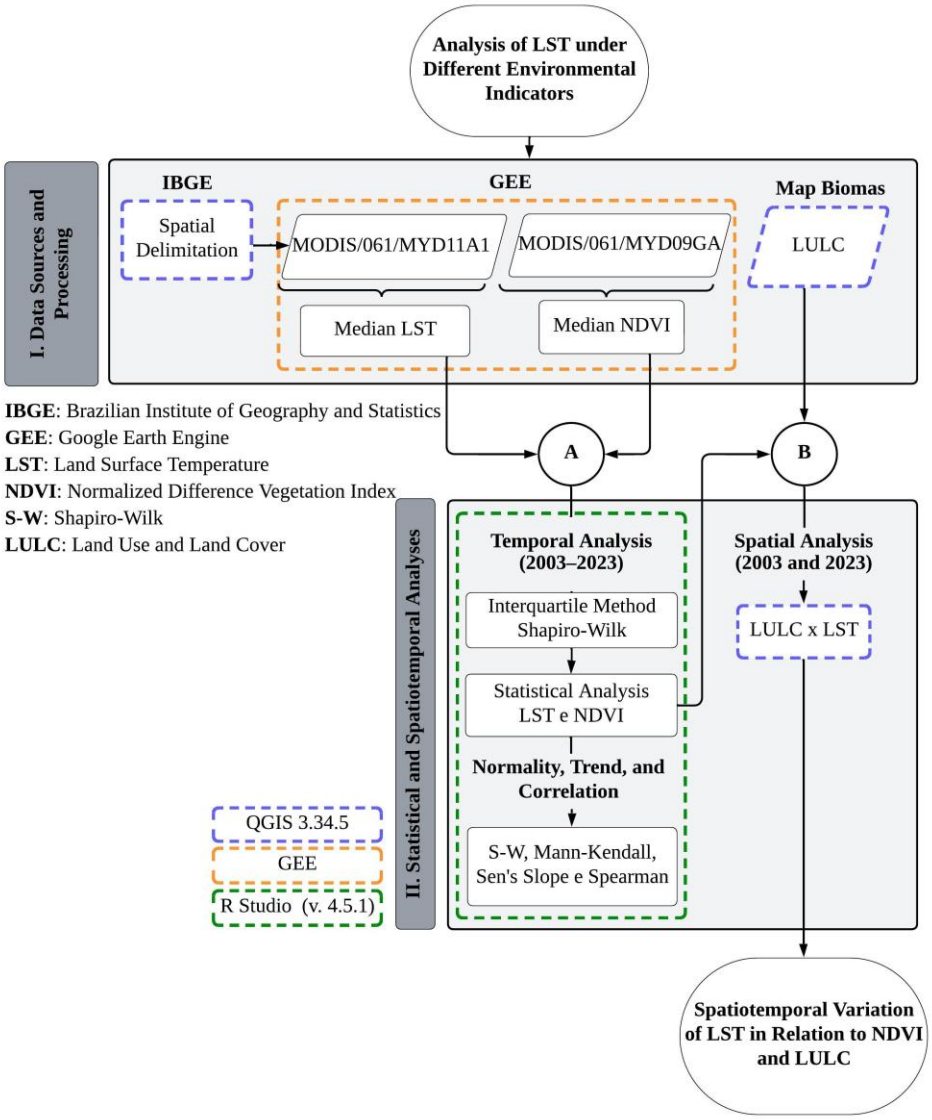

Figure 2 – Material and methods used for the study.

Base and data processing

The spatial localization of the municipality was delimited based on data from the Brazilian Institute of Geography and Statistics (IBGE), using the shapefile of municipalities in São Paulo State, from which the layer corresponding to the area of interest was extracted. The LST (Land Surface Temperature) was obtained from the MODIS/061/MYD11A1 product, converting the original Kelvin (K) values to Celsius degrees (°C). The NDVI (Normalized Difference Vegetation Index), used to identify the intensity of photosynthetic activity of the vegetation, was determined by the normalized ratio of the reflectance bands from the near-infrared (NIR) and red (RED), whose data were extracted from MODIS/061/MYD09GA (Renard et al., 2019).

ISSN eletrônico 2177-2738
RA'EGA, Curitiba, PR, V.65, n.1, p. 137–156, 4/2026
http://dx.doi.org/10.5380/raega.v65i1.103485

It is noteworthy that MODIS is aboard the Aqua satellite, with a temporal resolution of up to 2 days, and a pass time around 13:30 (local time) (Parkinson, 2022). The spatial resolution of the LST product is 1 km, while for surface reflectance data, used to determine NDVI, it is 500 m. Table 1 presents the equations and information for the MODIS bands used to determine LST and NDVI. MODIS data are available on the Google Earth Engine (GEE) platform, along with its quality control bands, which contain information about data collection conditions, such as cloud cover and sensor performance (Latorre et al., 2022). For this study, the QC_Day (LST) and state_1km (NDVI) bands were used.

Table 1 – Equations and information of MODIS bands (Aqua satellite) used to determine LST and NDVI.

Indicators	Equation		SF	MODIS Bands	λ (nm)
LST	$LST_{Day_{1KM}} - 273.15(°C)$	**(1)**	$2x10^{-2}$	LST_Day_1_KM (B31 e B32)	10.78-11.28 11.77-12.27
NDVI	$\frac{(NIR - RED)}{(NIR + RED)}$	**(2)**	$1x10^{-4}$	sur_refl_b01 sur_refl_b02	620-670 841-876

LST = Land Surface Temperature; NIR = *Near-Infrared*; SF = Scale Factor; B = Band; λ = Wavelength.

The time series of indicators was constructed with the median, a technique used to reduce the influence of extreme values in remote sensing data (Cai et al., 2017). This procedure is particularly useful to attenuate atmospheric interference or temporary sensor inconsistencies, as it is less sensitive to outliers than the mean (Kara; Yavuz, 2025). The heterogeneity of the landscape in the study area (e.g., urban areas, agriculture, and native vegetation) results in greater spectral and thermal variability of the pixels, reinforcing the need for this type of filtering. Furthermore, the adopted method does not assume normality in the data distribution, a condition verified by the Shapiro-Wilk (S-W) test (Shapiro; Wilk, 1965), which contributes to a stronger consistency and representativeness of the results and makes it appropriate for this type of analysis (Hekimoglu; Erdogan, 2013; Fernandes; Vicens; Furtado, 2018).

The LST values were evaluated in conjunction with the heat extremes observed in the study area. As a complementary analysis, daily Maximum Air Temperature (TMaxAr) data, organized in a continuous time series, were used. In the absence of the official climatological normal, the thermal extreme threshold was defined based on the 90th Percentile (P90) of TMaxAr, calculated seasonally using 15-day moving windows (±7 days around each day of the year), to represent the annual variability of the local climate. Extreme heat days were identified when the daily TMaxAr exceeded the respective P90. Thus, heat waves were defined as sequences of at least three consecutive days with TMaxAr above the P90, each sequence being considered a single event,

ISSN eletrônico 2177-2738
RA'EGA, Curitiba, PR, V.65, n.1, p. 137–156, 4/2026
http://dx.doi.org/10.5380/raega.v65i1.103485

regardless of its total duration. The monthly frequency of heat waves was determined based on the count of the number of events initiated each month. Months without occurrences were explicitly considered to ensure the temporal comparability of the results (Geirinhas et al., 2018; Oliveira et al., 2021).

For the spatial analysis of LULC changes associated with LST in the years 2003 and 2023, data from the MapBiomas Brasil project (Collection 9.0) were used, produced from Landsat images and classified using the Random Forest algorithm (Souza et al., 2020). These years were selected because they represent a 21-year time interval, sufficient to highlight significant changes in both the LULC pattern and the LST dynamics. The data processing, analysis, and integration steps used throughout the study were conducted on different computational platforms. Data processing to obtain LST and NDVI was performed on the GEE platform, developed for the storage, processing, and analysis of large geospatial data volumes. GEE offers a wide variety of remote sensing products and is used for spatial-temporal analyses at different geographic scales (Gorelick et al., 2017; Velastegui-Montoya et al., 2023). Statistical tests were conducted in the RStudio integrated development environment (version 4.5.1) (Posit, 2025), while the spatial analysis of LULC and LST were performed with the free QGIS software (version 3.34.5) (Dawson et al., 2025).

Statistical Analysis

The statistical and time series analysis (2003-2023) of the LST and NDVI indicators was performed after identifying and removing outliers, based on the Interquartile Range (IQR) method. The exclusion of these values aimed to minimize the influence of noise associated with residual atmospheric interference, cloud cover, shadows, or point inconsistencies in the sensor, which can introduce artificial peaks in the analyzed series and compromise the interpretation of spatial-temporal patterns. The IQR, defined as the difference between the upper and lower quartiles (Equations 1 and 2), was used to establish statistical limits and identify values that deviate from the typical dispersion of the data (Tukey, 1977). After applying this criterion, a visual analysis of the corresponding images was performed to confirm the non-representative nature of these values and justify its exclusion.

Equation 3: $Lower\ Limit = Q1 - (1.5 \times IQR)$
Equation 4: $Upper\ Limit = Q3 + (1.5 \times IQR)$

where: Q1 (1st Quartile) represents 25% of the data from the lower quartile; and Q3 (3rd Quartile) represents 75% of the data from the upper quartile; (1.5 x IQR) represents the "distance from the limit" to the lower and upper limits of the data.

ISSN eletrônico 2177-2738
RA'EGA, Curitiba, PR, V.65, n.1, p. 137–156, 4/2026
http://dx.doi.org/10.5380/raega.v65i1.103485

Thus, the LST time series was compared to NDVI values to understand the joint intra-annual variation of these indicators over the 21-year period. Initially, descriptive statistics were applied to verify the distributions and variability of the data. The temporal dynamics of LST and NDVI in the study area were analyzed based on simple linear regression, used to quantify the direction and magnitude of the indicators as a function of time. The coefficient of determination (R^2) was used to assess the fitness degree of this statistical model, which is widely used for climate studies associated with changes in the LULC (Kaiser et al., 2022; Mehmood et al., 2024).

Afterwards, the annual average of the LST and NDVI (from 2003 to 2023) was determined, with subsequent standardization within a range of 0 to 1. This procedure aimed to analyze the inter-annual variability of the indicators regarding their long-term relationships. The identification of increasing or decreasing trends in both daily time series and annual averages was performed using the Mann-Kendall (τ) test, while the magnitude of these trends was estimated with the Sen's Slope method. These non-parametric tests were selected because they do not require normality of the data, as verified by the S-W test (Shapiro; Wilk, 1965). The distribution of the data was also evaluated using frequency histograms. Additionally, the relation between LST and NDVI was verified using Spearman's correlation coefficient (ρ) and the Mann-Kendall Tau test (τ) (Mann, 1945; Bonnet; Wright, 2000; Hauke; Kossowski, 2011), adopting a significance level of 0.05 (α = 5%).

Finally, a spatial analysis of the annual average surface temperature (ST) for the years 2003 and 2023 was performed. For this, five LST classes were defined based on the temperature range of 18 °C to 30 °C: I) < 24 °C; II) 24-26 °C; III) 26-28 °C; IV) 28-30 °C; V) > 30 °C. This classification allowed each LST range to be associated with different types of LULC (classes defined by the MapBiomas project), as well as to identify spatial changes between 2003 and 2023, based on the difference in the total area occupied by each class.

III. RESULTS AND DISCUSSION

Temporal analysis of NDVI with LST

The LST time series (orange line) and NDVI (green line) obtained for the municipality of Itapetininga - SP for the period 2003 to 2023, whose LST thresholds were below 17.3 °C and above 42.5 °C, is presented in Figure 3. In addition, it is possible to observe seasonal patterns of both indicators, which show an inverse relationship over the years, based on linear regression (R^2 NDVI = 0.0404; R^2 LST = 0.0001).

ISSN eletrônico 2177-2738
RA'EGA, Curitiba, PR, V.65, n.1, p. 137–156, 4/2026
http://dx.doi.org/10.5380/raega.v65i1.103485

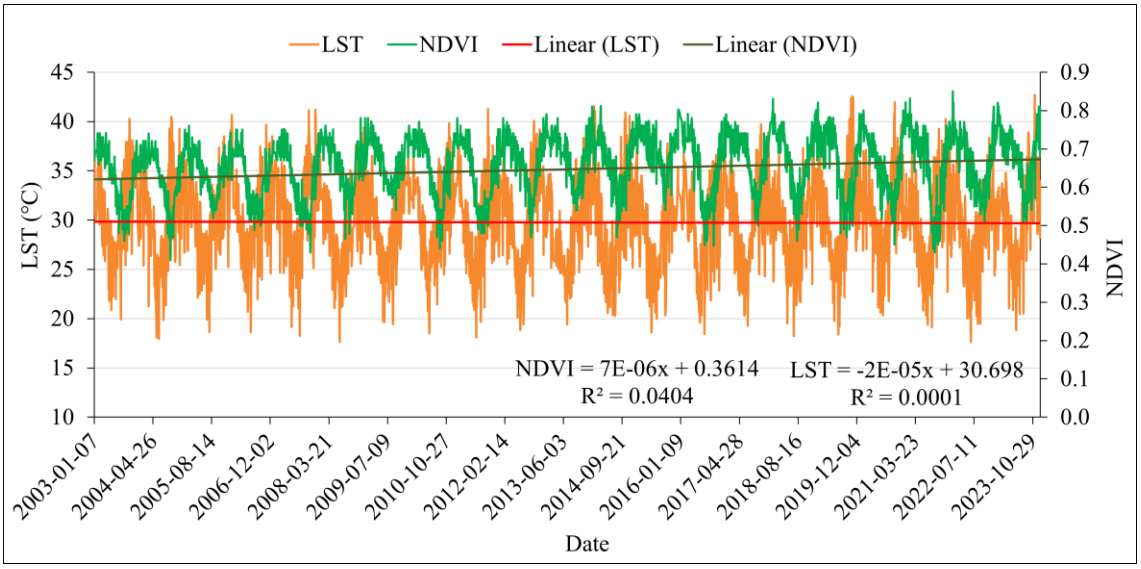

Figure 3 – Temporal series of indicators (LST and NDVI) for Itapetininga (2003–2023).

Table 2 presents the results of the descriptive statistics for LST and NDVI. NDVI maintained relatively high values throughout the series, with a range of 0.44. The range of NDVI values (0.41 to 0.85) indicates that, although there are areas with less vigorous vegetation, a scenario of stability in vegetation cover prevails, corroborated by the low standard deviation (0.07) compared to LST. Despite the observed seasonal oscillations, possibly associated with variations in water availability, there were no sharp drops in the values of this index, indicating a certain stability of vegetation cover throughout the analyzed period. The joint analysis of the indicators reinforces the influence of LULC in modulating local thermal dynamics. In this sense, the vegetation represented by NDVI confirms its regulatory effect to attenuate LST.

Table 2 – Descriptive statistics of indicators obtained for Itapetininga.

Statistics	LST (°C)	NDVI
Mean	29.77	0.64
Median	29.64	0.66
Mode	28.85	0.71
Variation coefficient	0.147	0.118
Standard deviation	4.36	0.07
Amplitude	24.79	0.44
Minimum	17.64	0.41
Maximum	42.43	0.85

Source: Authors (2025).

The statistical analysis of the data reveals important contrasts of thermal dynamics with vegetation cover in the study area. The surface temperature (ST) averaged 29.77 °C, with minimum values in winter (17.64 °C) and maximum values in summer (42.43 °C), resulting in a high thermal amplitude (24.79 °C). This variation

ISSN eletrônico 2177-2738
RA'EGA, Curitiba, PR, V.65, n.1, p. 137–156, 4/2026
http://dx.doi.org/10.5380/raega.v65i1.103485

reflects the strong influence of temporal variability (seasonal and inter-annual) associated with regional atmospheric conditions, such as the availability of solar radiation, the action of air masses, and cloud cover, which play a predominant role in modulating the LST. In this context, the LULC (Low Surface Temperature) acts as a complementary factor to the surface thermal response. The relatively high standard deviation (4.36 °C) also reinforces the temporal variability of the LST in the municipality.

From Figure 4, it is possible to interpret the distribution of LST and NDVI values. The histograms reinforce the results obtained by the descriptive statistics of LST and NDVI values. Thus, these values present defined distributions without significant asymmetries. LST is mainly concentrated in the 25 °C to 30 °C range, with a higher frequency around 29 °C, indicating moderate and relatively homogeneous thermal conditions in the analyzed area. NDVI, on the other hand, shows a greater predominance of values in the range of 0.55 to 0.75, with peaks near 0.65, suggesting moderate to high density vegetation cover. The S-W test indicated that both indicators analyzed presented distributions significantly different from the normal distribution (LST: W = 0.9971, p-value < 0.005; NDVI: W = 0.9804, p-value < 0.005), and justify the use of the non-parametric tests adopted.

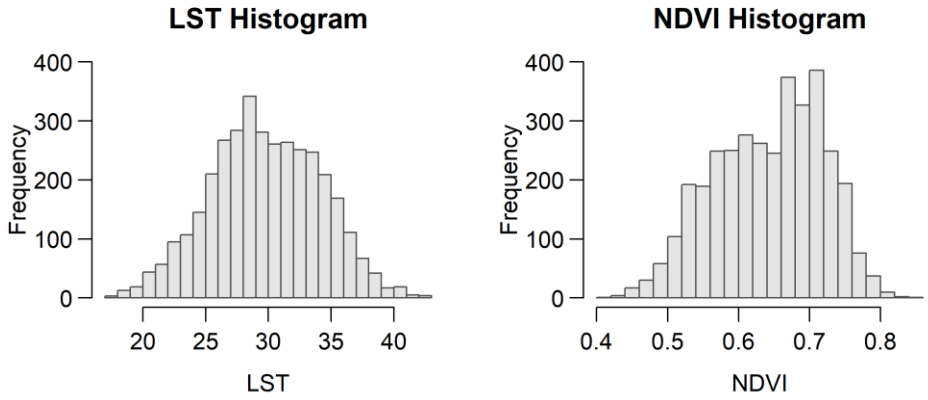

Figure 4 – Frequency histogram of LST and NDVI.

The LST time series showed no significant trend ($\tau = -0.0052$; p-value = 0.643), and the Sen's Slope was practically zero (-3.36×10^{-5}). In contrast, the NDVI time series showed a statistically significant increasing trend ($\tau = 0.1359$; p-value < 0.001), with a positive slope estimated by the Sen's Slope method (1.50×10^{-5}). Overall, an increase in NDVI values and a decline in LST values are observed during these 21 years of data, indicating thermal stability in the evaluated period, while vegetation cover showed a slight continuous increase.

It is also noteworthy that the high variability of the surface temperature (ST) in the municipality is not only linked to changes in the LULC (Low Limit Climate), but also to regional climatic factors. Figure 3 shows LST peaks in different years of the time series (2003, 2004, 2006, 2007, 2011, 2019, 2020 and 2023). According to

ISSN eletrônico 2177-2738
RA'EGA, Curitiba, PR, V.65, n.1, p. 137–156, 4/2026
http://dx.doi.org/10.5380/raega.v65i1.103485

information regarding meteorological phenomena in Brazil, available in Technical Notes from the National Institute of Meteorology (INMET, 2025), these elevations are also associated with extreme climatic events, especially the occurrence of heat waves that affected the São Paulo State. Figure 5 shows the frequency of extreme thermal event occurrences in Itapetininga, based on TempMaxAr (Maximum Air Temperature). It is observed that these events, which do not occur continuously throughout the analyzed period, exhibit strong inter-annual variability, with years practically free of occurrences (e.g., 2004, 2005, 2008) and years with high monthly recurrence (e.g., 2019, 2021, 2022, and 2023). Furthermore, an increase in the frequency of heat waves is observed from 2014 onwards. In addition, the events show a seasonal distribution, predominantly concentrated in the months of March to October.

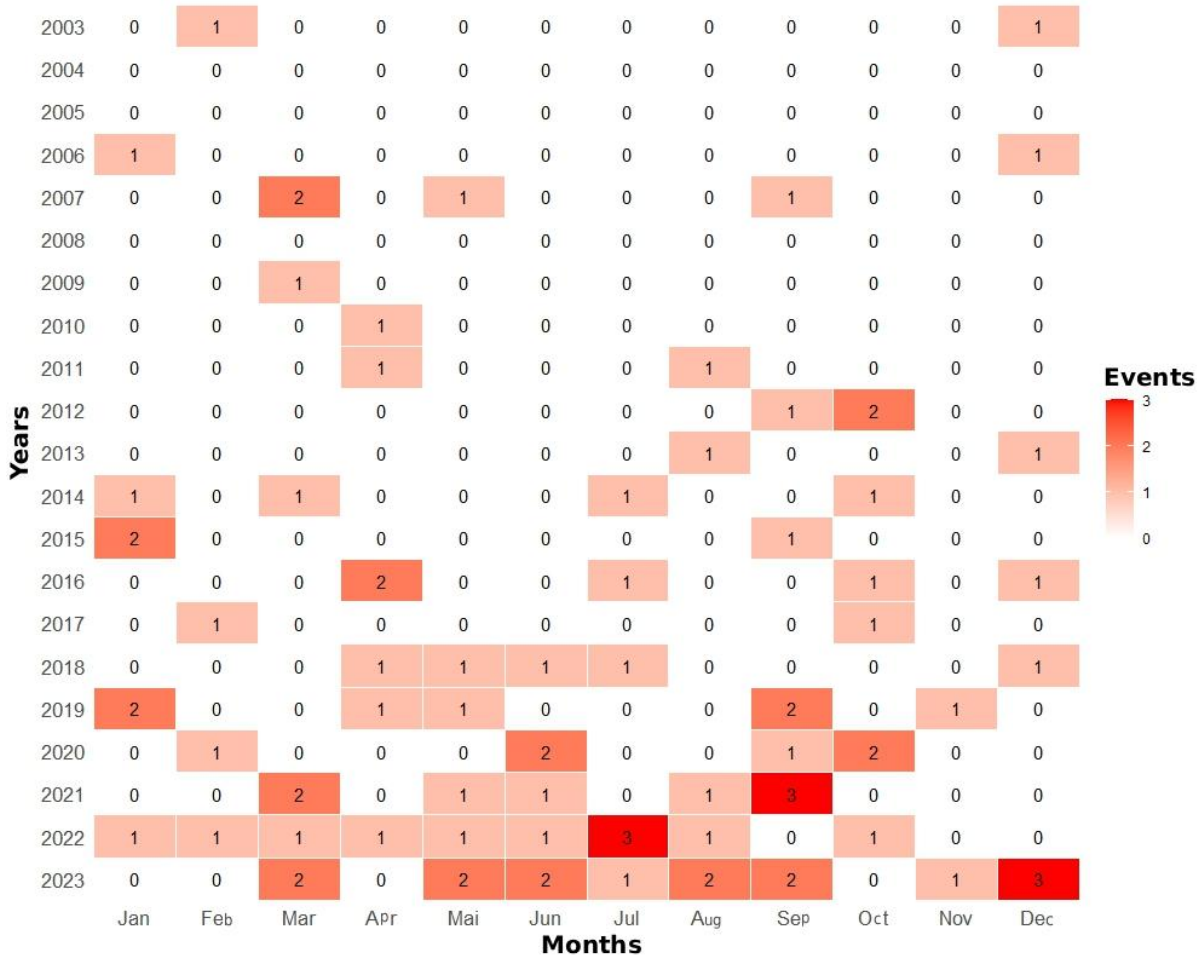

Figure 5 – Frequency of occurrence from extreme thermal events in the Itapetininga municipality.

The relationship between average annual surface temperature values and NDVI for the study area was evaluated using Spearman's (ρ) and Kendall's (τ) correlation coefficients (Figure 6). The results showed a statistically significant negative correlation ($\rho = -0.50$; $\tau = -0.36$; $\alpha < 0.05$), meaning that although the intensity

ISSN eletrônico 2177-2738
RA'EGA, Curitiba, PR, V.65, n.1, p. 137–156, 4/2026
http://dx.doi.org/10.5380/raega.v65i1.103485

of this relationship is moderate to weak, there is a tendency for LST to decrease as NDVI increases. This indicates that areas with greater vegetation cover presented milder surface temperatures, reinforcing the regulatory role of vegetation on local thermal dynamics.

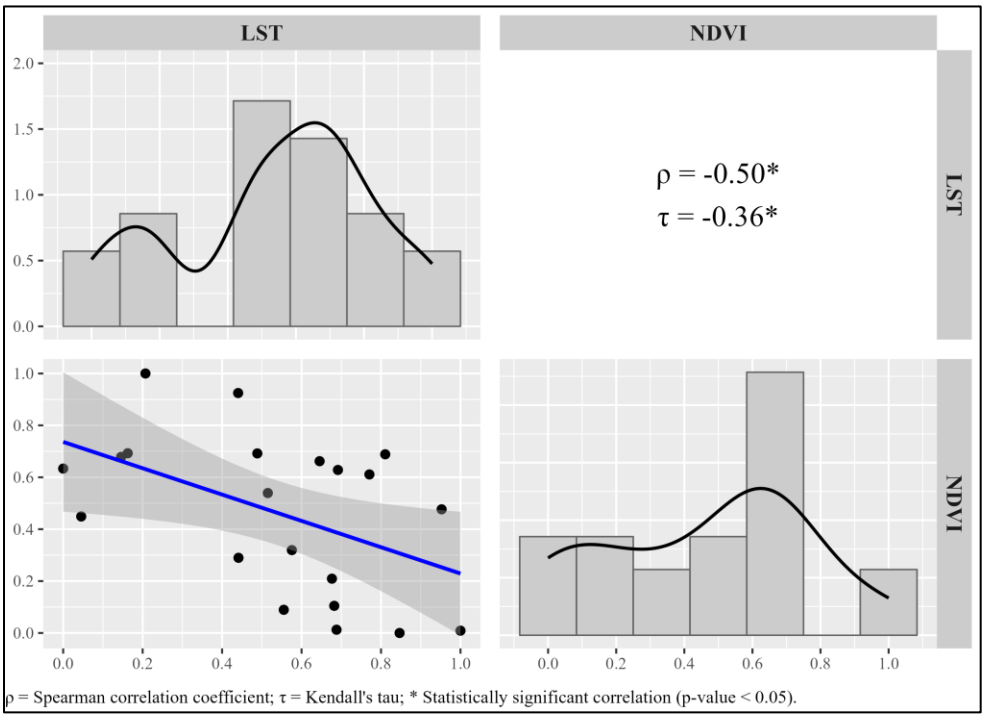

Figure 6 – Histogram and correlation coefficients of the annual averages from the indicators.

In this context, the results obtained in Itapetininga are consistent with the literature on the role of vegetation as a thermal regulator. Alavipanah et al. (2015), when analyzing the relationship between vegetation and urban surface temperature in Munich, Germany, highlighted the cooling effect promoted by vegetation, although a linear relationship is not established. Similarly, Zhang et al. (2020) observed that forest surfaces can have temperatures 1 °C to 2 °C below pasture areas, which highlights the relevance of vegetation cover to mitigate thermal extremes. According to the United States Environmental Protection Agency (EPA, 2025), urban areas characterized by a high concentration of buildings and low vegetation cover have daytime temperatures (0.5-2.1 °C) higher than peripheral areas. Thus, certain types of urban light-containing areas (LULC), such as parks, wooded areas, and water surfaces, can provide environments with more moderate temperatures.

Spatial analysis of LST with changes of LULC

The spatial analysis of LST in association with LULC shows modifications, mainly in the forest, pasture, agriculture, reforestation, and urbanized area classes. In 2003, the highest LST values were observed in the pasture and urbanized area classes, with a higher concentration in the North-South direction. In 2023, although

ISSN eletrônico 2177-2738
RA'EGA, Curitiba, PR, V.65, n.1, p. 137–156, 4/2026
http://dx.doi.org/10.5380/raega.v65i1.103485

the spatial configuration predominates, a reduction of the pasture class and an expansion of the agriculture class are observed (Figure 7). It is also noteworthy that, although LST values in the surrounding areas remain lower than in other regions of the study area, the maximum values were concentrated in the urban area, which expanded during the analyzed period.

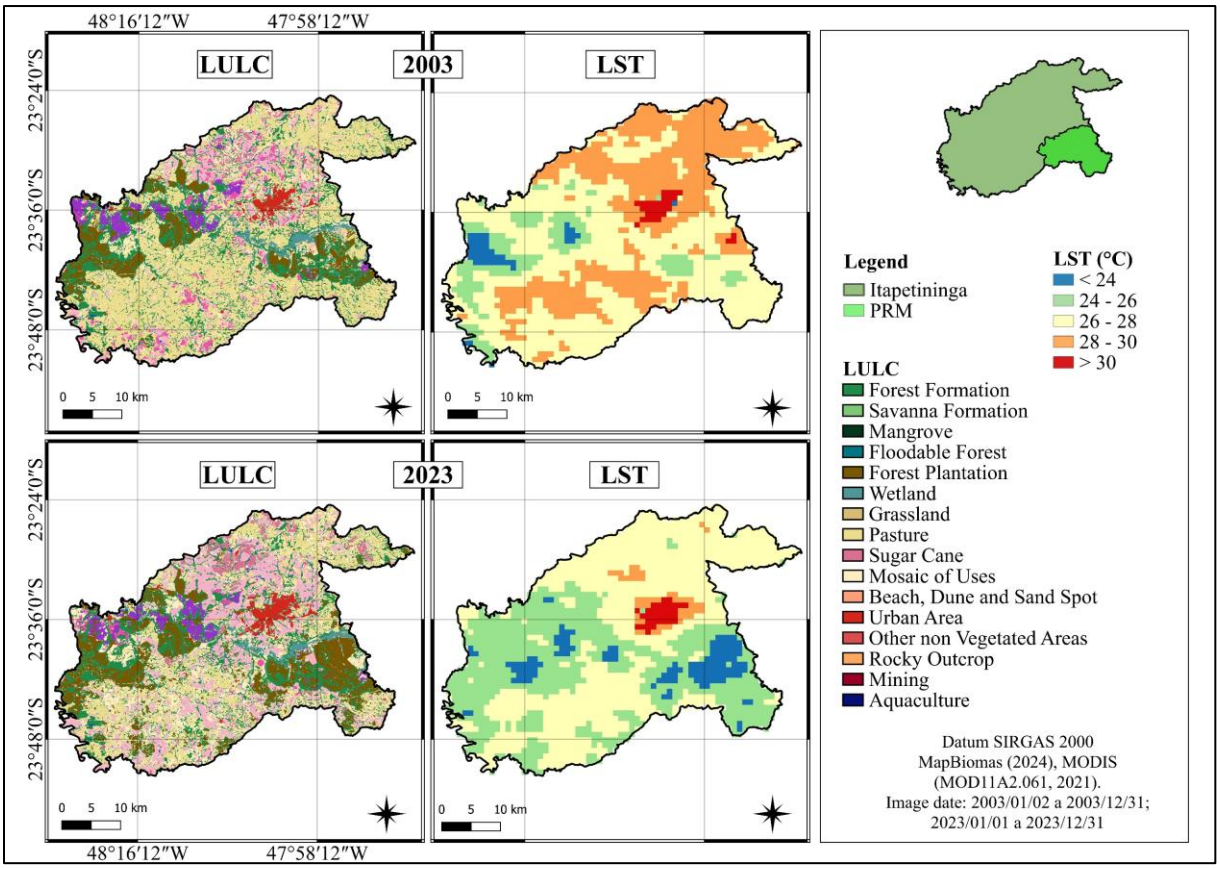

Figure 7 – Annual comparison of LST with LULC (2003 and 2023).

The results found corroborate the literature, such as those obtained by Aqdas et al. (2025), who analyzed the LULC and heat islands in Ghaziabad, India. The authors concluded that, throughout the study period, there was a decline in surface temperature within water bodies, vegetation, and agriculture, and a drastic increase in built-up areas. The main catalyst for this expansion of built-up areas is the gradual transition from rural to urban residential communities. Similarly, Głowienka and Kucza (2025) concluded that from 1990 to 2018, the interior of parks in Krakow, Poland, had, on average, temperatures 2 to 3 °C lower than the surrounding urbanized areas during late spring and summer. On the other hand, the reduction in surface temperature in 2023 is associated with the increase in areas classified as forest and reforestation, with an approximate decrease of 4 °C to 6 °C. This effect can be explained, in part, by the presence of the Itapetininga Experimental Station, located in the

ISSN eletrônico 2177-2738
RA'EGA, Curitiba, PR, V.65, n.1, p. 137–156, 4/2026
http://dx.doi.org/10.5380/raega.v65i1.103485

eastern part of the municipality, intended for experimental and commercial plantings of *Pinus elliottii*. Tree cover plays a fundamental role in thermal regulation by favoring shading and evapotranspiration (Coelho; Corrêa, 2013; Norton et al., 2015; Oke et al., 2017). This dynamic was also observed by Santos and Fialho (2024) in Viçosa/Minas Gerais State, where forest and reforestation areas concentrated the lowest LST, in contrast to pastures and consolidated urban areas.

Figure 8 shows the predominant classes of LULC and the difference between them (2003-2023). In 2003, the composition of LULC was characterized by 18.42% forest formation (of which 0.9% is represented by savanna formation) and 75.29% agro-pastoral (distributed in 39.26% pasture, 15.12% agriculture, 7.72% forestry and 13.19% other uses). While in 2023 there was an increase in the forest class, with 19.11% (comprising 0.7% savanna formation) and a decrease in the agro-pastoral class, with 74.67% (represented by 15.62% pasture, 23.98% agriculture, 13.72% forestry and 21.35% mosaic of different land uses). In this sense, the suppression of pasture gave way to forestry, soy and a mosaic of uses.

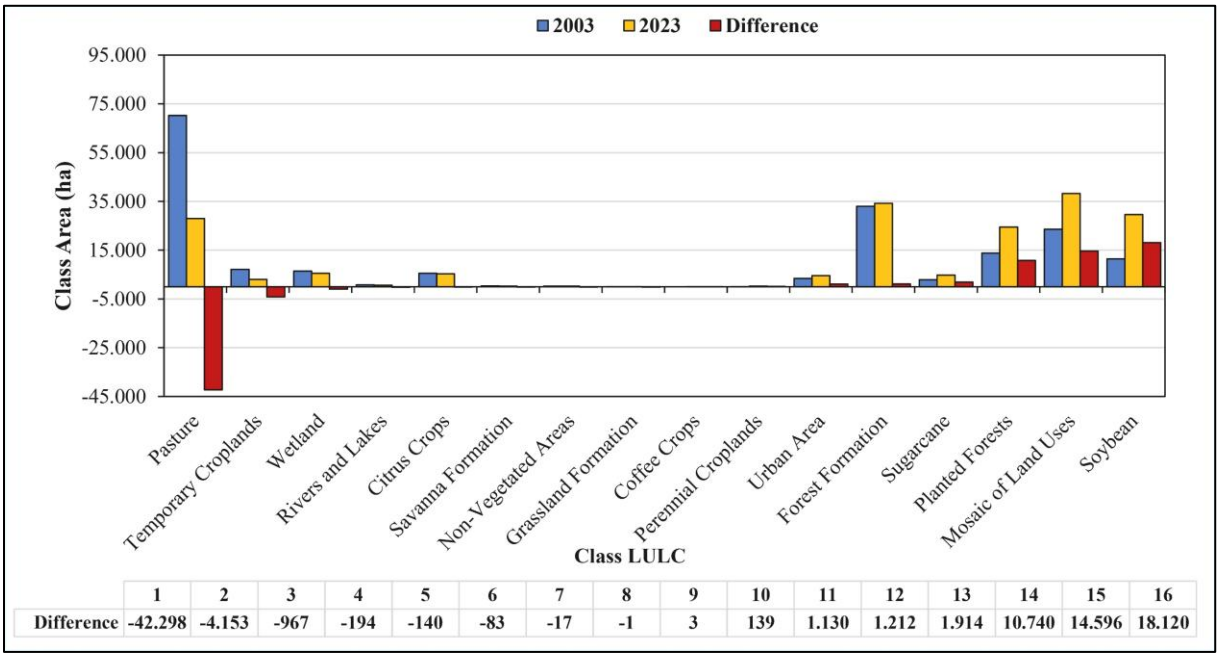

	1	2	3	4	5	6	7	8	9	10	11	12	13	14	15	16
Difference	-42.298	-4.153	-967	-194	-140	-83	-17	-1	3	139	1.130	1.212	1.914	10.740	14.596	18.120

Figure 8 – Area (ha) of LULC in 2003 and 2023 and the area difference (2023-2003).

Based on the results obtained, an expansion of 1,130 ha in urbanized areas was observed, accompanied by an increase of 1,212 ha in forest formation over the 21-year period. Similarly, the agriculture and forestry classes increased by 24,469 ha and 10,740 ha, respectively, while the pasture class showed a reduction of 42,298 ha. Regarding the LST obtained for the municipality of Itapetininga, a slight reduction of approximately 2 °C was observed of its values over the years analyzed, which can be attributed to the increase in the forest and forestry

ISSN eletrônico 2177-2738
RA'EGA, Curitiba, PR, V.65, n.1, p. 137–156, 4/2026
http://dx.doi.org/10.5380/raega.v65i1.103485

classes in the central region of the study area, especially on the banks of the Itapetininga River (Norton et al., 2015; Oke et al., 2017). This is visible when comparing the annual dynamics of LULC (Figure 6) with the time series of LST (Figure 3). However, agricultural and pasture areas remained in the 26-30 °C range, so that anthropic regions are characterized by high LST values (Maffioletti et al., 2021; Santos; Fialho, 2024).

Although Itapetininga shows accelerated growth in forestry, especially in the PRM area, a factor that contributes to the reduction of local surface temperature, it is not possible to affirm that this trend stems exclusively from the presence of this class. Other factors may also play a role in thermal regulation, such as hydrography, native vegetation, land use practices, relief, and atmospheric conditions. This uncertainty reinforces the need for studies that thoroughly evaluate the contribution of forestry to the local microclimate, considering both the growth and suppression periods of exotic species and its impacts on surface temperature.

IV. CONCLUSIONS

The analysis of LST in the Itapetininga municipality, over a 21-year data period (2003 to 2023), indicated a seasonal pattern in LST and NDVI values. Furthermore, an inverse and statistically significant correlation was found between these variables, indicating the local thermal regulation of tree vegetation. Additionally, the spatial distribution of LULC reinforces the importance of vegetation to mitigate the surface heat retention. In this context, the increase in forest and reforestation stood out as a relevant component to attenuate the LST in the years analyzed, although its specific contribution still requires more detailed investigation, especially due to variations resulting from the growth and cut phases. The results confirm that the integrated monitoring of LST, NDVI, and LULC is essential to understand the local thermal dynamics of climate change scenarios and LULC transformations. Future studies should consider complementary variables, such as the emissivity of different materials, topography, hydrography, and interaction with meteorological phenomena, to improve understanding of the mechanisms that regulate temperature and support territorial planning strategies aimed to mitigate the effects of climate change in the municipality.

Acknowledgments

The authors acknowledge the financial support from the Coordination for the Improvement of Higher Education Personnel (CAPES, No. 88887.210676/2025-00), the Foundation for Research Support of the Rio Grande do Sul State (FAPERGS, No. 23/2551-0001947-7), the National Council for Scientific and Technological

ISSN eletrônico 2177-2738
RA'EGA, Curitiba, PR, V.65, n.1, p. 137–156, 4/2026
http://dx.doi.org/10.5380/raega.v65i1.103485

Development (CNPq, No. 311977/2022-7 and 403696/2023-2), the Federal University of Santa Maria (UFSM), and the Geotechnologies Laboratory (LABGEOTEC).

V. REFERENCES

ALAVIPANAH, S.; WEGMANN, M.; QURESHI, S. et al. The role of vegetation in mitigating urban land surface temperatures: A case study of Munich, Germany during the warm season. Sustainability, v. 7, p. 4689–4706, 2015. DOI: https://doi.org/10.3390/su7044689.

AMORIM, M. C. C. T. Detecção remota de ilhas de calor superficiais: exemplos de cidades de porte médio e pequeno do ambiente tropical, Brasil. Finisterra, v. 52, n. 105, p. 111–133, 2017. DOI: https://doi.org/10.18055/Finis6888.

AQDAS, M.; USMANI, T. M; BENHIZIA, R.; SZABÓ, G. Urban Expansion and Thermal Stress: A Remote Sensing Analysis of LULC and Urban Heat Islands in Ghaziabad, India. Land. v. 14, n. 9, p. 1893, 2025. DOI: https://doi.org/10.3390/land14091893.

BONNET, D. G.; WRIGHT, T. A. Requisitos de tamanho de amostra para estimar correlações de Pearson, Kendall e Spearman. Psychometrika, v. 65, p. 23–28, 2000. DOI:10.1007/BF02294183.

CAI, Z.; JÖNSSON, P.; JIN, H.; EKLUNDH, L. Performance of smoothing methods for reconstructing NDVI time-series and estimating vegetation phenology from MODIS data. Remote Sensing., v. 9, n.12, p.1271, 2017. DOI: https://doi.org/10.3390/rs9121271.

COELHO, A. L. N.; CORREA, W. S. C. Temperatura de superfície Celsius do sensor TIRS/Landsat-8: metodologia e aplicações. Revista Geográfica Acadêmica, v. 7, n. 1, p. 31–45, 2013. DOI: https://doi.org/10.18227/1678-7226rga.v7i1.2996.

DAWSON, N. et al. qgis/QGIS: 3.44.5. Software, 2025. Disponível em: https://doi.org/10.5281/zenodo.17671248.

DIAS, M. A. F. S. Eventos climáticos extremos. Revista USP, São Paulo, n. 103, p. 33-40, 2014. Disponível em: https://pdfs.semanticscholar.org/b11f/16e5336755a04a865ba78e39cc622db60f2b.pdf.

EPA. What Are Heat Islands?. Washington: Environment Protection Agency, 2025.

FERNANDES, P. J. F.; VICENS, R. S.; FURTADO, L. F. de A. Comparação de algoritmos de filtragem em séries temporais de NDVI/MODIS. Revista Brasileira de Cartografia. v. 70, n. 3, p. 867–905, 2018. DOI: 10.14393/rbcv70n3-45705.

FLORES, J. L. R.; PEREIRA FILHO, A. J.; KARAM, H. A. Estimation of long-term low-resolution surface urban heat island intensities for tropical cities using MODIS remote sensing data. Urban Climate, v. 17, p. 32–66, 2016.

GEIRINHAS, J. L. et al. Characterizing the atmospheric conditions during the 2010 heatwave in Rio de Janeiro marked by excessive mortality rates. Science of The Total Environment, v. 650, p. 796-808, 2019. DOI: 10.1016/j.scitotenv.2018.09.060.

GŁOWIENKA, E.; KUCZA, M. Persistent Urban Park Cooling Effects in Krakow: A Satellite-Based Analysis of Land Surface Temperature Patterns (1990–2018). Remote Sensing. v. 17, n. 21, p. 3608, 2025. DOI: https://doi.org/10.3390/rs17213608.

ISSN eletrônico 2177-2738
RA'EGA, Curitiba, PR, V.65, n.1, p. 137–156, 4/2026
http://dx.doi.org/10.5380/raega.v65i1.103485

GORELICK, N. et al. Google Earth Engine: Planetary-scale geospatial analysis for everyone. Remote Sensing Environment. v. 202, p. 18–27, 2017. DOI: https://doi.org/10.1016/j.rse.2017.06.031.

HAUKE, J.; KOSSOWSKI, T. Comparison of Values of Pearson's and Spearman's Correlation Coefficients on the Same Sets of Data. Quaestiones Geographicae., v. 30, p. 87–93, 2011. DOI:10.2478/v10117-011-0021-1.

HEKIMOGLU S.; ERDOGAN B. Aplicação da abordagem da equação da mediana para detecção de outliers em redes geodésicas. Boletim de Ciências Geodésicas. v. 19, n. 4, p. 548-47, 2013. DOI: https://doi.org/10.1590/S1982-21702013000400002.

HENDGES, E. R.; FOLLADOR, F. A. C.; ANDRES, J. Correlation study between land use and covering with surface temperature registered by Landsat 8 satellite. Sociedade & Natureza, v. 32, p. 338–347, 2020. DOI: https://doi.org/10.14393/SN-v32-2020-42828.

HUNG, T.; UCHIHAMA, D.; OCHI, S. et al. Assessment with satellite data of the urban heat island effects in Asian mega cities. International Journal of Applied Earth Observation and Geoinformation, v. 8, n. 1, p. 34–48, 2006. DOI: 10.1016/j.jag.2005.05.003.

INSTITUTO BRASILEIRO DE GEOGRAFIA E ESTATÍSTICA – IBGE. Panorama — Itapetininga (SP). Cidades e Estados. Disponível em: https://cidades.ibge.gov.br/brasil/sp/itapetininga/panorama.

INSTITUTO NACIONAL DE METEOROLOGIA – INMET. Notas técnicas. Portal INMET. Disponível em: https://portal.inmet.gov.br/notasTecnicas.

IPCC. Climate Change 2023: Synthesis Report. Summary for Policymakers. Contribution of Working Groups I, II and III to the Sixth Assessment Report of the Intergovernmental Panel on Climate Change. Edited by Core Writing Team; H. Lee; J. Romero. Geneva: IPCC, 2023. 34 p.

ITAPETININGA. Plano Municipal de Desenvolvimento Rural Sustentável (PMDRS). Plano 2025-2028: São Paulo, 2025.

ITAPETININGA. Plano Municipal de Recuperação e Conservação da Mata Atlântica e Cerrado – PMMAeC. Itapetininga: Prefeitura Municipal; Instituto Cílios da Terra; Fundação SOS Mata Atlântica; Suzano S.A., 2023.

ITAPETININGA. Secretaria de Meio Ambiente, Infraestrutura e Logística (SEMIL). Guia de áreas protegidas: São Paulo, 2025.

KAISER, E. A.; ROLIM, S. B. A.; GRONDONA, A. E. B. et al. Spatiotemporal Influences of LULC Changes on Land Surface Temperature in Rapid Urbanization Area by Using Landsat-TM and TIRS Images. Atmosphere, v. 13, n. 3, p. 460, 2022. DOI: http://dx.doi.org/10.3390/atmos13030460.

KARA, Y.; YAVUZ, V. Urban Microclimates in a Warming World: Land Surface Temperature (LST) Trends Across Ten Major Cities on Seven Continents. Urban Science., v. 9, n. 4, p.115, 2025. DOI: https://doi.org/10.3390/urbansci9040115.

LATORRE, M. L.; ANDERSON, L. O.; SHIMABUKURO, Y. E. et al. SENSOR MODIS: CARACTERÍSTICAS GERAIS E APLICAÇÕES. Revista Espaço e Geografia, v. 6, n. 1, p. 91–121, 2022. DOI: 10.26512/2236-56562003e39720.

LIMA, K. C.; SATYAMURTY, P.; FERNÁNDEZ, J. P. R. Large-scale atmospheric conditions associated with heavy rainfall episodes in Southeast Brazil. Theoretical Applied Climatolology, v. 101, p.212-135, 2010.

LIU, W.; DONG, S.; ZHENG, J. et al. Quantifying the Rainfall Cooling Effect: The Importance of Relative Humidity in Guangdong, South China. J. Hydrometeor., v.23, p.875–889, 2022. DOI: 10.1175/JHM-D-21-0155.1.

ISSN eletrônico 2177-2738
RA'EGA, Curitiba, PR, V.65, n.1, p. 137–156, 4/2026
http://dx.doi.org/10.5380/raega.v65i1.103485

LOMBARDO, M. A. Ilha de Calor nas Metrópoles: o exemplo de São Paulo. São Paulo: Hucitec, 1985.

MAFFIOLETTI, F. D.; RAMALHO, A. H. C.; PAES, J. B.; FIEDLER, N. C. Influência da cobertura vegetal na temperatura da superfície. Agropecuária Científica no Semiárido, v. 17, n. 3, 29 dez. 2021. DOI: https://doi.org/10.30969/acsa.v17i3.1311.

MANN, H. B. Mann-Kendall. Non-Parametric Test against Trend. The Econometric Society, v. 13, p. 245–259, 1945.

MASHIKI, M. Y.; CAMPOS, S. Geoprocessamento aplicado na influência do uso e ocupação do solo na temperatura aparente da superfície no município de Botucatu/SP. Revista Energia na Agricultura, v. 28, n. 3, p. 143–149, 2013. DOI: https://doi.org/10.17224/EnergAgric.2013v28n3p143-149.

MEHMOOD, K.; ANEES, S. A.; MUHAMMAD, S. et al. Analyzing vegetation health dynamics across seasons and regions through NDVI and climatic variables. Scientific Reports, v. 14, n. 1, p. 1-22, 2024. DOI: http://dx.doi.org/10.1038/s41598-024-62464-7.

MERGA, B. B.; MOISA, M. B.; NEGASH, D. A. et al. Land Surface Temperature Variation in Response to Land-Use and Land-Cover Dynamics: A Case of Didessa River Sub-basin in Western Ethiopia. Earth Systems and Environment. v. 6, p. 803–815, 2022. DOI: 10.1007/s41748-022-00303-3.

MILANTONI, L.; TOLEDO, A. Mudanças do uso e cobertura da terra e sua relação com a variação de temperatura no município de Mogi das Cruzes SP. Enciclopédia Biosfera, v. 19, n. 40, 2022. DOI: 10.18677/EnciBio_2022B25.

NORTON, B. A.; COUTTS, A. M.; LIVESLEY, S. J. et al. Planning for cooler cities: a framework to prioritise green infrastructure to mitigate high temperatures in urban landscapes. Landscape and Urban Planning, v. 134, p. 127–138, 2015. DOI:10.1016/j.landurbplan.2014.10.018.

OKE, T. R.; MILLS, G.; CHRISTEN, A.; VOOGT, J. A. (Eds.). Urban Climates. Cambridge University Press, 2017.

OLIVEIRA, D. S. et al. Hotter, Longer and More Frequent Heatwaves: An Observational Study for the Brazilian City of Campinas, SP. Revista Brasileira De Meteorologia. v. 36, n. 2, p. 305–316, 2021. DOI: https://doi.org/10.1590/0102-77863620119.

PARKINSON, C. L. The Earth-Observing Aqua Satellite Mission: 20 years and counting. Earth and Space Science, v. 9, n. 9, p. 1–17, 2022. DOI: https://doi.org/10.1029/2022EA002481.

PORANGABA, G. F. O.; AMORIM, M. C. C. T. Geotecnologias Aplicadas à Análise de Ilhas de Calor de Superfície em Cidades do Interior do Estado de São Paulo. Revista Brasileira de Geografia Física, v. 12, n. 6, p. 2041–2050, 2019. DOI: 10.26848/rbgf.v12.6.p2041-2050.

POSIT TEAM. RStudio: Integrated Development Environment for R. Boston: Posit Software, PBC, 2025. Disponível em: http://www.posit.co/.

RAO, P. K. Remote sensing of urban "heat islands" from an environmental satellite. Bulletin of the American Meteorological Society. v. 53, p.647-648, 1972.

RENARD, F.; ALONSO, L.; FITTS, Y. et al. Evaluation of the Effect of Urban Redevelopment on Surface Urban Heat Islands. Remote Sensing. v. 11, n. 3, p. 299, 2019. DOI: https://doi.org/10.3390/rs11030299.

ROMERO, C. W. S.; SILVA, H. R.; MARQUES, A. P. et al. Relação entre as ilhas de calor e uso e ocupação do solo em centros urbanos de pequeno porte utilizando o sensoriamento remoto. Geociências, v. 39, n. 1, p. 253–268, 2020. DOI: https://doi.org/10.5016/geociencias.v39i1.14399.

ISSN eletrônico 2177-2738
RA'EGA, Curitiba, PR, V.65, n.1, p. 137–156, 4/2026
http://dx.doi.org/10.5380/raega.v65i1.103485

SANTOS, E. R. S.; TEIXEIRA, B. E. S.; ALMEIDA, E. C. et al. Análise da cobertura vegetal e da temperatura de superfície na região urbana e periurbana do município de Santarém/PA. Geosul, Florianópolis, v. 34, n. 71, p. 713-728, 2019. DOI: 10.5007/1982-5153.2019v34n71p713.

SANTOS, L. G. F.; FIALHO, E. S. Distribuição espacial da intensidade da ilha de calor de superfície no verão e inverno em Viçosa. Revista Ponto de Vista, v. 13, n. 1, 2024.

SOUSA, S. B.; FERREIRA, J. L. G. Relação entre temperatura de superfície terrestre, índices espectrais e classes de cobertura da terra no município de Goiânia (GO). RA'EGA - O Espaço Geográfico em Análise, v. 25, p. 75-99, 2012. DOI: https://doi.org/10.5380/raega.v26i0.30151.

SOUZA, C. M.; SHIMBO, J. Z.; ROSA, M. R. et al. Reconstructing three decades of land use and land cover changes in Brazilian biomes with Landsat archive and Earth Engine. Remote Sensing, v. 12, n. 17, p. 2735, 2020. DOI: https://doi.org/10.3390/rs12172735.

TUKEY, J. W. (Ed.). Exploratory data analysis. 1. ed. Addison-Wesley Publishing Company Reading, p. 668, 1977.

VELASTEGUI-MONTOYA, A.; MONTALVÁN-BURBANO, N.; CARRIÓN-MERO, P. et al. Google Earth Engine: A Global Analysis and Future Trends. Remote Sensing, v. 15, p. 3675, 2023. DOI: https://doi.org/10.3390/rs15143675.

XIONG, Y.; HUANG, S.; CHEN, F. et al. The Impacts of Rapid Urbanization on the Thermal Environment: A Remote Sensing Study of Guangzhou, South China. Remote Sensing, v. 4 n. 7, p. 2033-2056, 2012. DOI: https://doi.org/10.3390/rs4072033.

ZHANG, Q.; BARNES, M.; BENSON, M. et al. Reforestation and surface cooling in temperate zones: Mechanisms and implications. Global Change Biology, v. 26, n. 6, p. 3384–3401, 2020. DOI: 10.1111/gcb.15069.